

Surface Dynamics in Rubbed Polymer Thin Films Probed with Optical Birefringence Measurements

Alexander D. Schwab,[†] Dena Mae G. Agra,[‡] Jae-Hoon Kim,[‡] Satyendra Kumar,[‡] and Ali Dhinojwala^{*,†}

Department of Polymer Science, University of Akron, Akron, Ohio 44325, and Department of Physics and Liquid Crystal Institute, Kent State University, Kent, Ohio 44242

Received November 19, 1999; Revised Manuscript Received March 2, 2000

ABSTRACT: Measurements of the optical birefringence were used to probe the relaxation of rubbed ultrathin polystyrene (PS) films on glass substrates. It was found that the glass transition temperature, T_g , of the films dropped by 15–20 K as the film thickness decreased from 10 μm to 5.8 nm. Experiments on thick films ($\sim 10 \mu\text{m}$) revealed that molecules closer to the polymer–air interface relax more quickly than molecules farther from the interface. These results are explained in the context of past experimental studies of thermal properties of similar ultrathin polymer films.

Introduction

The influence of surfaces on the dynamics of thin polymer films has attracted significant attention in the past decade.^{1–18} Surface properties such as glass transition temperatures, liquid-crystal melting points, and surface mobility have important technological implications in the areas of adhesion, alignment of liquid crystals, and biocompatibility of polymers. A variety of experimental studies have established that surface–polymer interactions greatly influence the glass transition temperature (T_g) of ultrathin polymer films.^{1–6} These studies involved measurements of an average physical property such as film thickness using ellipsometry^{1–2,4} and X-ray reflectivity,^{5,6} or relaxation times using dielectric⁹ and optical probe techniques.¹⁰ These properties are found to be influenced by both the polymer–solid and the polymer–air interfaces. To address the effects of the polymer–air interface on a thin film's T_g , Forrest et al. have shown that free-standing films composed of polystyrene (PS) have a very dramatic decrease (of 70 K) in T_g as the film thickness approaches polymer molecule dimensions.^{3,4} The drop in T_g for free-standing films has been explained by higher mobility at the polymer–air interface compared to that in the bulk. Other experiments on supported films reveal either an increase^{2,5,6} or a decrease^{1–4,9} in thin film T_g relative to the bulk T_g . This increase or decrease depends on the influence of both the polymer–air interface as well as the chemical composition of the polymer and the supporting solid substrate.

The dramatic drop in T_g observed in free-standing films is puzzling. Although initial AFM results on polymer–air surfaces indicate rubbery properties of surface layers,¹⁶ more recent experimental results have shown very small or negligible changes in surface polymer properties.^{8,18} Experiments using near-edge X-ray absorption fine-structure (NEXAFS) on rubbed polystyrene films have shown almost no difference in the rate of relaxation between polymer chains within 1 nm of the surface and chains within 10 nm of the

surface, again indicating a small influence of the surface on the system's dynamics.¹⁸ On the other hand, Monte Carlo simulations have shown a higher mobility at polymer–air surfaces, due to a reduction in density.¹⁷ However, this effect does not extend more than a few segmental diameters into the film. The objective of the present work is to understand the reason for these contradictory effects of the polymer–air interface on polymer mobility.

The strategy used in our experiments to probe polymer–air surfaces was inspired by earlier NEXAFS work on rubbed polymer surfaces.^{18,19} The rubbing process induces orientational order in polymer chains, and the relaxation of this order provides a sensitive probe of the relaxation process of the surface chains.^{18,20} Although NEXAFS has excellent molecular sensitivity, it lacks a high enough signal-to-noise ratio to do rapid kinetic measurements of relaxation dynamics. On the other hand, past results have shown that the rubbing process also induces birefringence in polyimide films.²¹ We have found that the birefringence technique requires inexpensive instrumentation and offers excellent sensitivity to probe relaxation at polymer surfaces and in thin films.

In this paper we report results of two generic experiments. One involves rubbing various thicknesses of PS films on glass substrates and measuring the relaxation of the birefringence as a function of temperature while heating the rubbed film at a predetermined constant rate. These data are modeled to determine the T_g of the composite thin films. The second set of experiments involves rubbing a 10 μm thick cast PS film with different rubbing strengths. The lighter we rub, the more localized the perturbation of the polymer–air interface, and the observed relaxation rates are, therefore, mostly of the surface chains. Our results indicate that the T_g of a PS film of thickness comparable to the radius of gyration (R_g) is 15–20 K lower than the bulk. Very similar drops in T_g were seen for the polymer–air interface of thick cast PS films. This drop in T_g is much smaller than that observed for free-standing films.^{3,4} These results are discussed in light of previously published results.

[†] University of Akron.

[‡] Kent State University.

* To whom correspondence should be addressed.

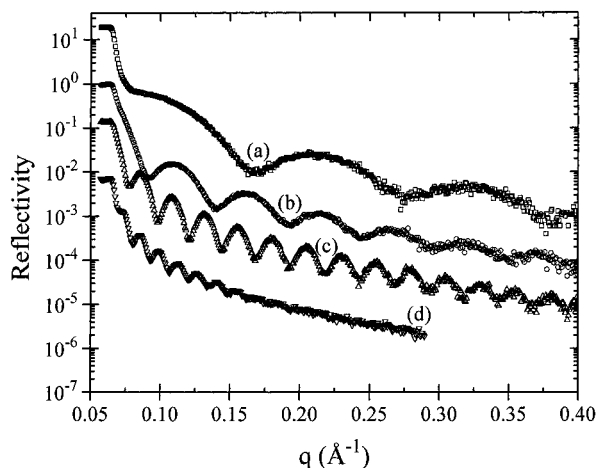


Figure 1. X-ray specular reflectivity profiles of spin-coated PS films of different thickness. The curves have been shifted vertically for clarity. The data were fit to the reflectivity equation to determine the film thicknesses of (a) (□) 5.8 nm, (b) (○) 12.5 nm, (c) (△) 28.0 nm, and (d) (▽) 48.0 nm.

Experimental Section

Sample Preparation. All polymer films used in this study are of PS with a weight-average molecular weight of 48 500 g mol⁻¹ and a polydispersity index of 1.03. Glass substrates were cleaned by soaking them in a sulfuric acid and Nochromix solution for roughly 24 h, rinsing thoroughly with deionized water from a Millipore Milli-Q water purifying system, and drying with nitrogen gas. Polystyrene films with thickness $h \leq 115$ nm were prepared by spin-coating different concentration solutions of polymer in toluene at various spinning speeds. To create films with much greater thicknesses (~ 10 μm), a film-casting technique was used wherein a concentrated solution of PS in toluene was poured onto a glass substrate, and the substrate was then placed in a closed container to control the rate of solvent evaporation. The spin-coating and film-casting solutions were prepared by dissolving the PS in HPLC grade toluene as received from Aldrich. Twenty-four hours was allowed for complete dissolution of the polymer before filtering the solutions twice using 0.45 μm PTFE filters. The spin-coated samples were allowed to dry under vacuum conditions for 24 h before X-ray reflectivity measurements were performed. Twenty-four hours was considered to be enough for complete removal of the solvent given the diffusion constant of toluene in polystyrene and the extremely small thicknesses of the films.²² The spin-coated samples for birefringence measurements were annealed for 5 min in an oven set at 105 °C to remove residual birefringence created by the spinning process and to remove thermal history. The samples were then cooled to room temperature outside the oven. The cast films were dried at 110 °C for 2–3 h in a vacuum before the birefringence measurements were made.

Thickness Measurements. The thickness of the PS films was determined by X-ray reflectivity (XRR) measurements using a Cu K α line on a Rigaku 18 kW rotating anode with four-circle Huber goniometer.²³ For a film of thickness d and X-ray refractive index n , the reflectivity R is written as

$$R(q) = \left| \frac{r_{\text{af}} + r_{\text{fs}} \exp(inqd)}{1 + r_{\text{af}} r_{\text{fs}} \exp(inqd)} \right|^2$$

where $q = (4\pi/\lambda) \sin \theta$ is the X-ray momentum transfer along surface normal, and r_{af} and r_{fs} are the X-ray reflectances at the air–film and film–substrate interfaces, respectively.²⁴ The interference of waves reflected from the two interfaces generates Kiessig fringes which provide accurate measurements of the film thickness, electron density gradients, and the vertical rms roughnesses at the two interfaces. XRR curves for different films are shown in Figure 1. The sharp Kiessig fringes indicate

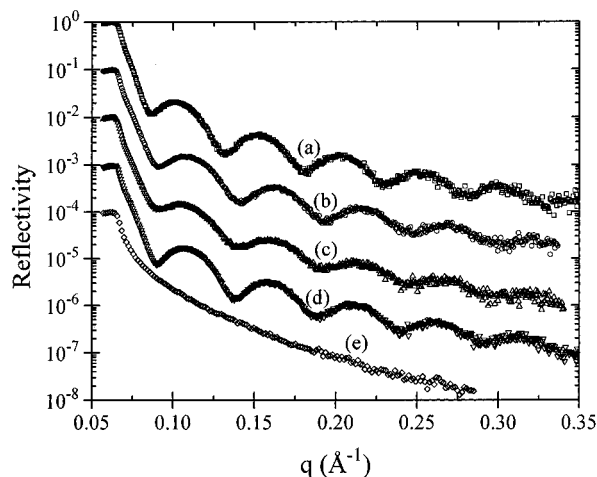


Figure 2. X-ray reflectivity profiles of 12.5 nm thick PS film on glass substrate at room temperature: (a) (□) before annealing, (b) (○) after annealing for 5 min at 105 °C, (c) (△) after the film was rubbed at room temperature, (d) (▽) after the birefringence experiment, and (e) (◇) after several hours of heating at 105 °C. The curves have been shifted vertically for clarity.

uniform films. Film thickness was determined by the least-squares fit of $R(q)$ to the reflectivity data.

To ensure that the annealing process did not cause the PS film to dewet and that the rubbing process did not significantly change the film thickness, XRR measurements were performed on a 12.5 nm film, shown in Figure 2. The relative invariance of the fringe pattern measured before a birefringence experiment (unannealed) up to the completion of the experiment indicates that the film thickness remained constant within the experimental error of 0.5 nm throughout the sample preparation and the experiment. Fringes became less sharp upon rubbing compared to the film after the birefringence experiment. This indicates an increase in surface roughness of the film upon rubbing, which subsequently disappears after heating. The final reflectivity curve in Figure 2, without any Kiessig fringes, is indicative of dewetting. This only occurred when the film was kept for several hours at 105 °C.

Birefringence Measurements. Optical retardation measurements were done using a He–Ne laser with a photoelastic modulator (PEM90, Hinds Instruments) placed between crossed polarizers.²⁵ The PEM's optic axis was kept at 45° to the axes of the polarizer and the analyzer. The rubbed samples were mounted in a heating stage (Mettler) for controlled heating (1 K min⁻¹) and placed between the PEM and analyzer such that the rubbing direction was perpendicular to the optic axis of the PEM. A collimated beam of light from a He–Ne laser source was incident normal to the substrate. The signal from the photodetector placed after the analyzer was fed to a lock-in amplifier (EG & G Princeton Applied Research, model 5210) tuned to the 50 kHz signal from the PEM.

PS samples were rubbed gently with a velvet cloth. It has previously been shown that the rubbing process induces alignment of the PS chains.¹⁸ Since PS has a negative stress–optical coefficient, this results in a negative birefringence and is dominated by the alignment of the benzyl side groups perpendicular to the direction of rubbing. Rubbing is not a quantitative process, and for the measurements of the effects of thickness on T_g , the samples were rubbed repeatedly until a few additional rubbing attempts no longer observably increased the birefringence of the film. Though it is possible to further increase the birefringence of the film through many more subsequent rubbings, this was not performed because of the damage that may have been caused to the thin films. Films rubbed in this manner are described as being rubbed to saturation throughout this paper. Studies were also conducted to determine the effects of the degree of rubbing on the observed T_g , by rubbing films to different extents.

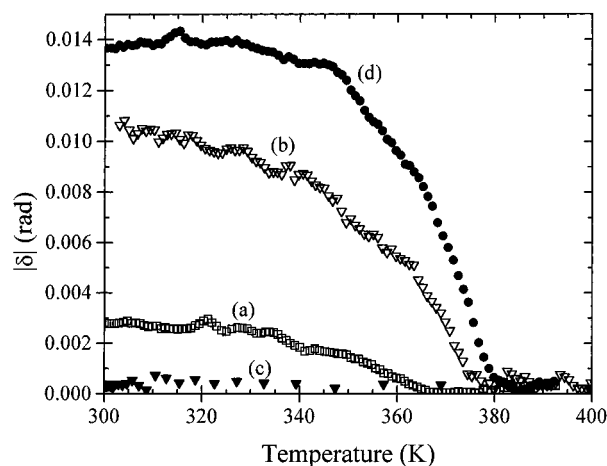


Figure 3. Decay of phase retardation as a function of temperature of rubbed PS films of various thicknesses: (a) (□) 5.8 nm during heating, (b) (▽) 48.0 nm heating, (c) (▼) 48.0 nm on cooling after the first heating cycle, and (d) (●) cast film heating. All the samples were heated at 1 K min⁻¹, and cooling rates were uncontrolled.

Though the rubbing process is known to cause alignment of polymer chains by applying a stress to them, it has also been shown to create a grooved surface. It was recently suggested that the birefringence of rubbed surfaces is dominated by the "form birefringence" associated with the roughness of the surface.²⁶ A theoretical formulation based on uniform grooves predicts a positive birefringence for rubbed films.²⁴ The birefringence of the PS films used in this study was found to be negative, indicating that the form birefringence was negligible, and the reorientation dynamics probed in this paper are therefore associated with the changes in the orientation of PS chains.

Results and Discussion

Relaxation as a Function of Film Thickness. The decay of birefringence of three films rubbed to saturation upon heating is shown in Figure 3. The initial retardation is progressively higher for thicker films simply because there is a larger number of chains present that align upon rubbing. On heating the rubbed samples, the retardation decreases monotonically to zero at temperatures above the T_g of the films. To demonstrate that the measured decrease in retardation is associated with the disorientation in rubbed films, consider the retardation of the 48.0 nm film as it is cooled from 400 K after the first heating cycle, shown in Figure 3. The retardation remains low, indicating that the decrease in retardation of a rubbed sample is due to a permanent randomization of the chain alignment.

To illustrate the differences in relaxation dynamics as a function of film thickness, the data for the cast and the 5.8 nm films are replotted after normalization in Figure 4. The retardation $|\delta|$ has been normalized by the initial retardation of the film $|\delta_i|$. The retardation completely vanishes by the time the temperature reaches 365 K for the 5.8 nm film and 385 K for the cast film. Evidently, the thinner films show faster mobility, indicating a reduction in T_g . Since the rate of relaxation is a strong function of the heating rate and the physical properties of the polymer layer, further quantitative analysis of the relaxation dynamics requires a physical model which we discuss below.

Relaxation Model. In analogy to past work, we have developed a phenomenological description of polymer

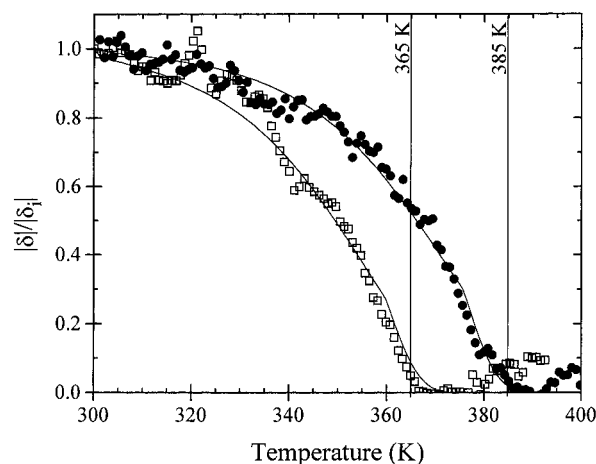


Figure 4. Normalized retardation curves comparing relaxation dynamics between a (□) 5.8 nm film and a (●) cast film upon heating. The solid lines through the data are from fits using the relaxation model discussed in the text. The third fitting parameter was used where ΔE and β are fixed at -205 kJ mol⁻¹ and 0.36, respectively. The T_g was determined to be 357 K for the 5.8 nm film and 372 K for the cast film.

relaxation using the Kohlrausch–Williams–Watts (KWW) relaxation equation²⁷ with an Arrhenius temperature dependence below T_g and a Williams–Landel–Ferry (WLF) temperature dependence²⁸ above T_g . On the basis of the KWW model, the time dependence of the birefringence at a constant temperature is given by the following equation:

$$\Delta n(t) = \Delta n(0) \exp\left[-\left(\frac{t}{\tau}\right)^\beta\right] \quad (1)$$

where $\Delta n(t)$ is the birefringence at time t , $\Delta n(0)$ is the initial birefringence (i.e., at $t = 0$), τ is the relaxation time at the temperature of interest, and β is the relaxation exponent. The exponent, β , is related to the distribution of relaxation times in the sample. When $\beta = 1$, a single relaxation time exists, and eq 1 reduces to a simple exponential decay. When $\beta < 1$, a distribution of relaxation times exists with a long tail of high-frequency relaxations. Equation 1 in its current form cannot be used to fit the data because the experiments were not performed at constant temperature.

The rate of change of the birefringence at a given time and temperature can be determined by taking the derivative of eq 1:

$$\frac{d(\Delta n)}{dt} = \frac{-\Delta n \beta t^{\beta-1}}{\tau^\beta} \quad (2)$$

Here, it can be seen that the rate of change of birefringence depends only on the magnitude of the birefringence, the relaxation time, and the relaxation exponent at time t . Integration of eq 2 with respect to time yields

$$\Delta n(t) = \Delta n(0) \exp\left[-\int_0^t \frac{\beta t^{\beta-1}}{\tau^\beta} dt\right] \quad (3)$$

The relaxation time is known to be temperature dependent. It is therefore necessary to establish a relationship between the experimental time and the experimental temperature. Since, in this study, the sample is heated at a constant rate, the relationship between time and temperature is taken to be linear:

$$T = T_0 + At$$

where T_0 is the starting temperature and A is the heating rate. By incorporating this temperature–time relationships into eq 3, one obtains

$$\Delta n(T) = \Delta n(T_0) \exp \left[- \int_{T_0}^T \frac{\beta (T - T_0)^{\beta-1}}{(A\tau(T))^\beta} dT \right] \quad (4)$$

The relaxation time below T_g is a function of both temperature and physical aging effects, if any. In this model, we have not taken into account physical aging and use a simple Arrhenius relationship to model the temperature dependence below T_g . Above T_g , a WLF temperature dependence is used as shown in eqs 5a and 5b.

$$\tau(T) = \tau_0 \exp \left(- \frac{\Delta E}{RT} \right) \quad T < T_g \quad (5a)$$

$$\log \left(\frac{\tau(T)}{\tau(T_g)} \right) = \frac{-c_1(T - T_g)}{c_2 + T - T_g} \quad T > T_g \quad (5b)$$

where τ_0 represents the preexponential time constant, ΔE is the activation energy, R is the Rydberg gas constant $8.315 \text{ J mol}^{-1} \text{ K}^{-1}$, $\tau(T_g)$ is the relaxation time at the glass transition temperature, and c_1 and c_2 are WLF parameters for PS taken from the literature to be 13.7 and 50.0 K, respectively.²⁹ The temperature of interest in this study is the glass transition temperature. If we define the glass transition temperature in such a way that at T_g the relaxation time is $\tau(T_g)$, then eqs 5a and 5b become

$$\tau(T) = \tau(T_g) \exp \left[- \frac{\Delta E}{R} \left(\frac{1}{T} - \frac{1}{T_g} \right) \right] \quad T < T_g \quad (6a)$$

$$\tau(T) = \tau(T_g) \times 10^{[-c_1(T - T_g)]/[c_2 + T - T_g]} \quad T \geq T_g \quad (6b)$$

This same temperature dependence for the relaxation time has been seen experimentally.³⁰

In this study, we have defined the glass transition temperature to be the temperature where $\tau(T) = \tau(T_g)$. Experimental measurements of relaxation times in PS at T_g include dielectric relaxation measurements ($\tau(T_g) \sim 0.5 \text{ s}$),³¹ photon correlation spectroscopy studies ($\langle \tau \rangle_{T_g} = 71.6 \text{ s}$ with $\beta = 0.38$ and $\langle \tau \rangle_{T_g} = 34 \text{ s}$ with $\beta = 0.4$)^{32,33} and a study observing the reorientation of second harmonic chromophores ($\langle \tau \rangle_{T_g} = 40 \text{ s}$ with $\beta = 0.24$).³⁰ The relationship between the average relaxation time at T_g , $\langle \tau \rangle_{T_g}$, the KWW relaxation exponent β , and the relaxation time $\tau(T_g)$ is

$$\tau(T_g) = \frac{\langle \tau \rangle_{T_g} \beta}{\Gamma(1/\beta)} \quad (7)$$

assuming that the relaxation dynamics follow a KWW time dependence. Using eq 7, $\tau(T_g)$ can range between 0.5 and 20 s.^{30–33} In this study, we chose $\tau(T_g) = 5 \text{ s}$ as the definition for the glass transition temperature. This choice of $\tau(T_g)$ yields T_g 's for the cast films, considered to behave like bulk PS, of $\sim 370 \text{ K}$, which is comparable to the T_g for PS of 378 K as determined using differential scanning calorimetry. Although the choice of $\tau(T_g)$ is somewhat arbitrary, and a different choice of $\tau(T_g)$ would yield a different T_g upon fitting the data,

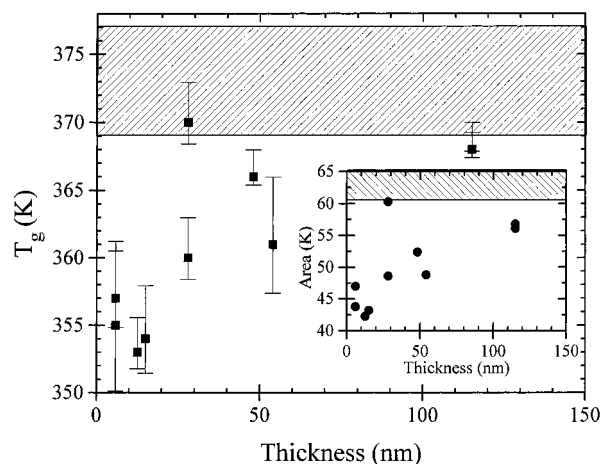


Figure 5. T_g as a function of film thickness. The solid squares are the T_g values obtained using the third fitting method described in the text. The error bars reflect the uncertainty of the fits. The shaded region represents the T_g with uncertainty for the cast films ($\sim 10 \mu\text{m}$ thick). The inset is a plot of the area under the normalized relaxation curves for films of different thicknesses.

the overall trends seen in T_g remain unchanged regardless of the choice of $\tau(T_g)$ within the range 0.5–20 s.

In the first series of experiments, films with thicknesses of 5.8, 12.5, 15.0, 28.0, 48.0, 54.0, 115 nm, and $\sim 10 \mu\text{m}$ were rubbed to saturation, and birefringence measurements were performed to obtain relaxation curves. In the second series of experiments, a single cast film was rubbed to different extents, and birefringence relaxation measurements were performed for each rubbing strength. Equation 4 was then used to fit the birefringence relaxation curves to determine ΔE , β , and T_g . Any depth dependence of the relaxation time or relaxation exponent was neglected. All reported values of ΔE , β , and T_g are therefore averages over the film depth perturbed by rubbing. This depth is described in more detail later in the paper.

Analysis of the fitted parameters yields no apparent thickness or rubbing strength dependence of β or ΔE , with a mean ΔE of $-202 \pm 34 \text{ kJ mol}^{-1}$ and a mean β of 0.38 ± 0.05 where the error is the standard deviation of all the fits. Experimentally determined activation energies for relaxations in PS below T_g lie in the range -188 to -209 kJ mol^{-1} .³⁰ The T_g 's determined from this first fitting procedure decreased with decreasing film thickness. A second fitting procedure was used where β was fixed at 0.36, yielding fits with errors equivalent to those of the first fitting procedure. This fitting procedure yielded a mean ΔE of $-207 \pm 28 \text{ kJ mol}^{-1}$ and a decreasing trend of T_g with decreasing film thickness. A third and final fitting procedure was used wherein ΔE was fixed at -205 kJ mol^{-1} and β was fixed at 0.36. Errors from the fits using this final procedure were acceptable, but not as good as the previous two procedures. This is most likely due to the fact that there is only one adjustable parameter in the last fitting procedure as opposed to two and three adjustable parameters in the previous two procedures. Examples of relaxation data fit using the third fitting procedure appear in Figure 4.

T_g as a Function of Film Thickness. Figure 5 displays the glass transition temperatures as a function of film thickness for PS films of various thicknesses rubbed to saturation. The points represent the T_g values determined using the third fitting procedure. The error

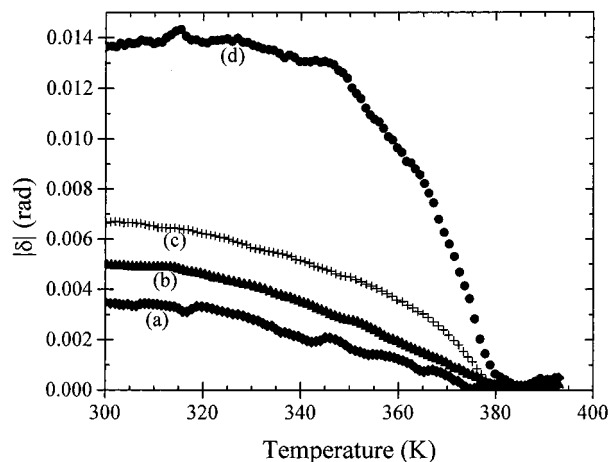


Figure 6. Relaxation of retardation of cast films rubbed to different degrees as a function of temperature: (a) (♦) rubbed three times, (b) (▲) rubbed six times, (c) (+) rubbed nine times, and (d) (●) rubbed to saturation. All the samples were heated at 1 K min⁻¹.

bars reflect the uncertainty of the fitting procedure to determine T_g . The shaded region of the plot represents the uncertainty for the T_g 's of the cast film (thickness $\sim 10 \mu\text{m}$). The cast films show T_g 's (372 K) that are very similar to those measured using DSC and other dynamic techniques (378 K). Films with thicknesses greater than 30 nm have T_g 's that lie within 10 K of the T_g of the cast films. On the other hand, the 5.8 and 12 nm films have T_g 's that lie 15–20 K below the T_g of the cast films.

The inset of Figure 5 is a plot of the area under the normalized relaxation curves for the films of different thicknesses. The area decreases with film thickness, meaning the relaxation dynamics become faster with decreasing film thickness. Regardless of the relaxation model used to quantify the film dynamics, the increasing rate of relaxation with decreasing film thickness is still apparent.

Relaxation as a Function of Rubbing Strength.

In liquid crystal display applications, rubbing has been used as a technique to induce alignment of liquid crystal molecules. In a series of experiments by van Aerle et al., polyimide films of various thicknesses were rubbed in a controlled manner, and the optical retardation of these films was measured. Significant evidence was found showing that the depth of penetration increased as the rubbing pressure or rubbing density is increased.²¹ The exact depth dependence of the refractive index is not known. Regardless of the refractive index depth profile, the total retardation for a film can be expressed as follows:

$$|\delta| = \int_0^h 2\pi \Delta n(z) dz / \lambda \quad (8)$$

where $\Delta n(z)$ is the birefringence at a distance z from the surface, h is the overall film thickness, and λ (=632.8 nm) is the wavelength of light used.

Since it has been shown that the penetration depth is a function of the rubbing strength, we can use it to investigate the influence of the penetration depth on the relaxation dynamics. The relaxation of birefringence in a single cast film rubbed to different strengths was measured. The cast film was annealed for 30 min at 110 °C after each run to erase thermal history. The relaxation curves for this can be seen in Figure 6. The strongly rubbed samples have a higher initial retardation,

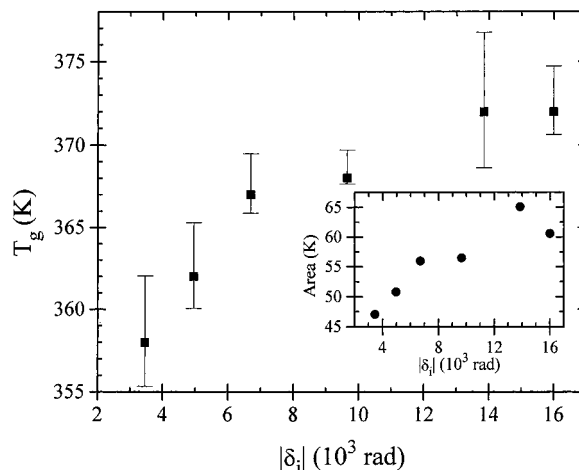


Figure 7. T_g determined by fitting retardation curves of cast films rubbed to different degrees. Symbols and error bars are determined as in Figure 7. The x -axis is the initial retardation before relaxation at time = 0. The lowest $|\delta_i|$ value corresponds to $d_{\text{eff}} > 7 \text{ nm}$, and the largest corresponds to $d_{\text{eff}} > 32 \text{ nm}$. The inset is a plot of the area under the normalized relaxation curves.

tion, as expected. Also, the rate of relaxation is faster for the lightly rubbed sample. This implies that polymer molecules at the polymer–air surface are much more mobile than the interior molecules, indicating the T_g 's for thin films in Figure 5 are strongly influenced by the polymer–air interface. It can also be argued that by increasing the rubbing strength we may be probing molecules of a highly stretched nature exhibiting nonlinear relaxation times. If that were the case, we would expect faster relaxation times as a function of rubbing, not the opposite trend observed in this study. The rates of relaxation, however, must be determined more quantitatively.

Equations 4, 6a, and 6b were used to fit relaxation curves obtained for thick PS films rubbed to different degrees. Glass transition temperatures determined from these fits can be found in Figure 7. On the horizontal axis is plotted the initial retardation, $|\delta_i|$, as an indicator of the extent of rubbing. The initial retardation is proportional to the effective depth of rubbing, d_{eff} , which is explained in the following paragraph. Samples with large rubbing depths have higher T_g 's than samples with lower rubbing depths. This essentially means that molecules farther from the PS–air interface relax more slowly than molecules closer to the surface. The inset of Figure 7, a plot of the area under the normalized relaxation curves as a function of initial birefringence, supports the same conclusion.

To estimate a lower limit for d_{eff} , some simplifying assumptions must be made in eq 8. The most important of these assumptions is that the alignment is uniform to a depth d_{eff} . This model is similar to a model proposed by van Aerle et al. (model IV) where rubbing orients the film uniformly to a depth d_0 (called d_{eff} in this paper), with a tail of nonuniform orientation extending to a greater depth, d_1 .²¹ Ignoring the effect of this tail of orientation as an approximation, eq 8 reduces to a product of $(2\pi/\lambda)|\Delta n|d_{\text{eff}}$. To determine $|\Delta n|$, we assume that the polymer molecules in the thinnest film studied, $h = 5.8 \text{ nm}$, are uniformly aligned throughout the entire depth of the film. By setting $d_{\text{eff}} = 5.8 \text{ nm}$, $|\Delta n|$ is calculated to be 0.048 on the basis of the initial retardation. The next assumption is to use this value of $|\Delta n|$ to

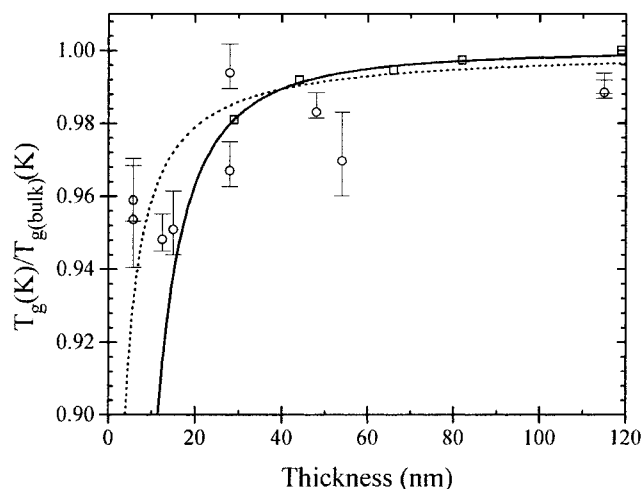


Figure 8. Comparison of T_g (K)/ $T_{g(\text{bulk})}$ (K) as a function of film thickness with previously published results: (○) this study, (□) Forrest et al. (supported films),⁴ (solid line) Keddie et al.,¹ and (dotted line) Fukao et al.⁹

determine the lower limit for d_{eff} in the cast films rubbed to different strengths. This assumption was determined to be valid by van Aerle et al., who found the Δn value in their model to be the same regardless of the rubbing pressure or the rubbing density used to align their polyimide films.²¹ For this reason, d_{eff} is only an approximation and at worst represents a lower limit for the penetration depth. The actual depth of penetration is larger than d_{eff} .

On the basis of these assumptions, we find the lower limit for the d_{eff} 's starting with the leftmost point in Figure 7 of 7, 10, 14, 20, 28, and 32 nm. Van Aerle and co-workers found similar penetration depths of 10–60 nm for rubbed polyimide films.²¹ The reduction in T_g by 15–20 K for $d_{\text{eff}} \sim 7$ nm is in good agreement with the results for the thinnest film data in Figure 5, indicating a strong influence of the polymer–air interface on the dynamics of ultrathin films. The relaxation data from the cast films rubbed to different strengths indicate the presence of a more mobile layer near the polymer–air interface. As films become thinner, this mobile surface becomes a larger fraction of the film's total volume, leading to faster dynamics.

Comparison with Previous Works. The results displayed in Figure 5 show that the T_g of a PS film on glass drops 20 K from bulk T_g as the film thickness approaches 5.8 nm. Our results are compared with results from the past works^{1,4,9} for PS films in Figure 8. The solid lines in Figure 8 are best fits to the data obtained from two separate studies.^{1,9} The PS films used in the study performed by Keddie et al.¹ were supported on etched silicon as opposed to the aluminum-coated glass substrates used by Fukao et al.⁹ It should be noted that the results presented in Figure 8 by Forrest et al. are ellipsometric studies of PS films supported on SiO₂-coated silicon substrates unlike the studies of the freely standing PS films.⁴ The solid line in Figure 8 as determined by Keddie et al.¹ becomes an extrapolation for thicknesses below 13 nm, where significant deviations between it and the supporting data begin to occur. For film thicknesses greater than 13 nm, the results of the three studies agree well. All of these investigations suggest that the T_g of the polymer film is not significantly affected (to within 2%) until the film thickness falls below 20–30 nm. In contrast, Wu and co-workers

have reported an increase in T_g for PS on silicon substrates by 60 K for films as thick as 40 nm.⁵

The reduction in T_g by 20 K for a lightly rubbed surface of a thick (cast) film indicates that the polymer–air surface is more mobile than in the bulk. In comparison, results from free-standing PS films by Forrest et al.^{3,4} observe a large reduction in T_g (by 70 K) when film thickness falls below 70 nm for a film composed of 767 000 g mol⁻¹ PS. The same study found that the film thickness at which the T_g drops is molecular weight dependent, with a higher molecular weight polymer having a larger thickness for the T_g drop. This suggests that the effect of the free surface extends roughly 35 nm into the film. In this study, the rubbing strength dependence of the T_g suggests that the free surface effect penetrates to a depth of greater than 15 nm into the PS film. This agrees to within an order of magnitude with the free-standing film studies; however, the magnitude of change observed by the birefringence measurements on supported films are far lower than in free-standing films.

The results of this study indicate that a polymer's mobility increases with decreasing film thickness. This does not agree qualitatively with many diffusion measurements in the literature. For example, Hall and Torkelson find that the diffusion of fluorescent probes in PS films at 376 K decreases roughly by an order of magnitude as the film thickness decreases from 560 to 80 nm.¹¹ The substrate used in that study was quartz, which has surface properties similar to that of glass. Measurements by Rafailovich and co-workers find that PS diffusion at 426 K is slowed roughly by 2 orders of magnitude near a bounding Si surface relative to the diffusion far from the surface.¹³ Diffusion measurements by Frank et al. showed that the lateral diffusion at 413 K of fluorescent labeled polymer chains decreases by a factor of 2 as the film thickness decreases from 200 to 60 nm.¹² Solely on the basis of the diffusion measurements alone, one would arrive at the conclusion that a polymer's mobility should decrease as the film thickness decreases. Furthermore, the reasons for such long-range effects on diffusion constants are not clear and require further investigation.

The work reported here is for PS on glass, a non-attractive surface. Previous results on different polymer–substrate systems have been controversial. Studies of poly(methyl methacrylate) (PMMA) films on SiO₂ surfaces reveal that the T_g of PMMA increases ~ 3 K relative to the bulk T_g as film thicknesses approach 5 nm.² In the same study, it was found that the T_g of a PMMA film on a gold-coated substrate drops ~ 7 K as film thickness approaches 30 nm.² Also, Wu and co-workers have measured a 20–50 K increase in the T_g of poly(2-vinylpyridine) (PVP) films on silicon oxide for films as thin as 8 nm.⁶ It is believed that the increase in T_g seen for PMMA films on SiO₂ and for PVP films on SiO₂ is due to a strong polar interaction between the polymer and the substrate, causing decreased polymer molecule mobility. This polar interaction is not present in the PS–SiO₂ system and hence the decrease in T_g observed in this study and the studies of Keddie et al.,¹ Forrest et al. (supported films),⁴ and Fukao et al.⁹ Studies of attractive polymer–surface systems are currently underway using the birefringence technique.

Conclusions

This paper introduced a simple and inexpensive technique to probe polymer relaxation in ultrathin films.

Observations of the relaxation of PS films of different thicknesses supported on glass have provided significant evidence of faster relaxations in thinner films. Analysis of the data reveals a 15–20 K drop in T_g as film thickness decreased from 10 μm to 5.8 nm with most of the decrease in T_g occurring at thicknesses below 25 nm. This drop in T_g correlates well with previous results on similar systems.^{1,4,9} Experiments performed on thick ($\sim 10 \mu\text{m}$) films revealed that PS chains within 15 nm of the polymer–air interface relaxed significantly faster than in the bulk, causing a drop of 20 K in T_g . The high mobility of polymer chains at the free surface is undoubtedly responsible for the enhanced mobility observed for ultrathin films of PS on glass.

Acknowledgment. We gratefully acknowledge funding from the 3M Corporation (Young Faculty award to A.D.), the Lord Corporation (Graduate Fellowship to A.S.), NSF S&T Center ALCOM DMR 89-20147 (S.K. and D.M.G.A.), and the NSF–CAREER Award (A.D.) for this work. We also thank Dr. Jutta Luettmer-Strathmann for her help with the relaxation model.

References and Notes

- (1) Keddie, J. L.; Jones, R. A. L.; Cory, R. A. *Europhys. Lett.* **1994**, *27*, 59.
- (2) Keddie, J. L.; Jones, R. A. L.; Cory, R. A. *Faraday Discuss.* **1994**, *98*, 219.
- (3) Forrest, J. A.; Dalnoki-Veress, K.; Stevens, J. R.; Dutcher, J. R. *Phys. Rev. Lett.* **1996**, *77*, 2002.
- (4) Forrest, J. A.; Dalnoki-Veress, K.; Dutcher, J. R. *Phys. Rev. E* **1997**, *56*, 5705.
- (5) Wallace, W. E.; van Zanten, J. H.; Wu, W. L. *Phys. Rev. E* **1995**, *52*, R3329.
- (6) van Zanten, J. H.; Wallace, W. E.; Wu, W. L. *Phys. Rev. E* **1996**, *53*, R2053.
- (7) Lin, E. K.; Kolb, R.; Satija, S. K.; Wu, W. L. *Macromolecules* **1999**, *32*, 3753.
- (8) Xie, L.; DeMaggio, G. B.; Frieze, W. E.; DeVries, J.; Gidley, D. W. *Phys. Rev. Lett.* **1995**, *74*, 4947.
- (9) Fukao, K.; Miyamoto, Y. *Europhys. Lett.* **1999**, *46*, 649.
- (10) Hall, D. B.; Hooker, J. C.; Torkelson, J. M. *Macromolecules* **1997**, *30*, 667.
- (11) Hall, D. B.; Torkelson, J. M. *Macromolecules* **1998**, *31*, 8817.
- (12) Frank, B.; Gast, A. P.; Russell, T. P.; Brown, H. R.; Hawker, C. *Macromolecules* **1996**, *29*, 6531.
- (13) Zheng, X.; Rafailovich, M. H.; Sokolov, J.; Strzhemechny, Y.; Schwarz, S. A.; Sauer, B. B.; Rubinstein, M. *Phys. Rev. Lett.* **1997**, *79*, 241.
- (14) Li, Z.; Tolan, M.; Höhr, T.; Kharas, D.; Qu, S.; Sokolov, J.; Rafailovich, M. H.; Lorenz, H.; Kotthaus, J. P.; Wang, J.; et al. *Macromolecules* **1998**, *31*, 1915.
- (15) Wang, J.; Tolan, M.; Seeck, O. H.; Sinha, S. K.; Bahr, O.; Rafailovich, M. H.; Sokolov, J. *Phys. Rev. Lett.* **1999**, *83*, 54.
- (16) Kajiyama, T.; Tanaka, K.; Takahara, A. *Polymer* **1998**, *39*, 4665.
- (17) Mansfield, K. F.; Theodorou, D. N. *Macromolecules* **1991**, *24*, 6283.
- (18) Liu, Y.; Russell, T. P.; Samant, M. G.; Stöhr, J.; Brown, H. R.; Cossy-Favre, A.; Diaz, J. *Macromolecules* **1997**, *30*, 7768.
- (19) Toney, M. F.; Russell, T. P.; Logan, J. A.; Kikuchi, H.; Sands, J. M.; Kumar, S. K. *Nature* **1995**, *374*, 709.
- (20) Wei, X.; Zhuang, X.; Hong, S. C.; Goto, T.; Shen, Y. R. *Phys. Rev. Lett.* **1999**, *82*, 4256.
- (21) van Aerle, N. A. J. M.; Barmantlo, M.; Hollering, R. W. J. *J. Appl. Phys.* **1993**, *74*, 3111.
- (22) Gall, T. P.; Kramer, E. J. *Polymer* **1991**, *32*, 265.
- (23) Cull, B.; Shi, Y.; Kumar, S.; Shih, R.; Mann, J. *Phys. Rev. E* **1995**, *51*, 526.
- (24) Born, M.; Wolf, E. *Principles of Optics*, 6th ed.; Pergamon Press: New York, 1980.
- (25) Kim, J.-H.; Kumar, S.; Lee, S.-D. *Phys. Rev. E* **1998**, *57*, 5644.
- (26) Kim, J. H.; Rosenblatt, C. *Appl. Phys. Lett.* **1998**, *72*, 1917.
- (27) Kohlrausch, R. *Ann. Phys. (Leipzig)* **1847**, *12*, 393. Williams, G.; Watts, D. C. *Trans. Faraday Soc.* **1971**, *66*, 800.
- (28) Williams, M. L.; Landel, R. F.; Ferry, J. D. *J. Am. Chem. Soc.* **1955**, *77*, 3701.
- (29) Ferry, J. D. *Viscoelastic Properties of Polymers*, 3rd ed.; Wiley and Sons: New York, 1980.
- (30) Dhinojwala, A.; Wong, G. K.; Torkelson, J. M. *J. Chem. Phys.* **1994**, *100*, 6046.
- (31) Saito, S.; Nakajima, T. *J. Appl. Polym. Sci.* **1959**, *2*, 93.
- (32) Lee, H.; Jamieson, A. M.; Simha, R. *Macromolecules* **1979**, *12*, 329.
- (33) Lindsey, C. P.; Patterson, G. D.; Stevens, J. R. *J. Polym. Sci., Polym. Phys. Ed.* **1979**, *17*, 1549.

MA9919514